State of the Art in Nuclear Medicine Dose Assessment

Michael G. Stabin, PhD, CHP, and A. Bertrand Brill, MD, PhD

Basic calculational methods and models used in dose assessment for internal emitters in nuclear medicine are discussed in this overview. Methods for quantification of activity in clinical and preclinical studies also are discussed, and we show how to implement them in currently available dose calculational models. Current practice of the use of internal emitters in therapy also is briefly presented here. Some of the future challenges for dose assessment in nuclear medicine are discussed, including application of patient-specific dose calculational methods and the need for significant advances in radiation biology.
Semin Nucl Med 38:308-320 © 2008 Elsevier Inc. All rights reserved.

Radiation dose assessment for internal emitters in nuclear medicine has risen from its humble beginnings in the 1940s, when researchers used a single 3-factor equation to estimate organ dose, to its current practice, in which researchers are using complex and sophisticated electronic models and image-based methods to calculate organ doses and dose distributions in nuclear medicine patients. Standardized dose estimates are needed for basic risk/benefit decision-making for diagnostic agents, which continue to be used and to proliferate at a rapid rate. More individually tailored dose calculations are required for therapy agents, which also are undergoing rapid development for use against various forms of cancer and other diseases. In this article, we will describe the current state of the art in nuclear medicine dosimetry. Some review of historical literature will be provided, but our focus will be on the current state of practice and on the widely anticipated implementation of patient-specific dose calculations, which is currently not generally routine in clinical practice.

Basic Dose Calculational Methods: Equations

The evaluation of dose from radiopharmaceuticals begins with the evaluation of absorbed dose, which is the energy

deposited per unit mass in human tissues. The units for expressing this quantity are Gy (1 J/kg) or rad (100 erg/g = 0.01 Gy). We will show later, however, that a complete understanding of dose and effect in therapeutic applications may require the evaluation of a different dose quantity. The earliest formulations of dosimetry systems were given by Marinelli and coworkers and Quimby and Feitelberg[1,2] and gave the dose from a beta emitter that decays completely in a given organ or tissue as:

$$D_\beta = 73.8\ C\ E_\beta\ T$$

where D_β is the beta dose in rad, C is the concentration of the nuclide in the tissue in microcuries per gram, E_β is the mean energy emitted per decay of the nuclide, T is the half-life of the nuclide in the tissue, and the factor 73.8 is a unit conversion factor.

A more complete generic equation for the absorbed dose rate for an organ assumed to be uniformly contaminated with radioactivity may be shown as:

$$\dot{D}_T = \frac{k\ A_S \sum_i y_i\ E_i\ \phi_i(T \leftarrow S)}{m_T}$$

where $\dot{D}_T$ = absorbed dose rate to a target region of interest (Gy/sec or rad/h), A_S = activity (MBq or μCi) in source region S, y_i = number of radiations with energy E_i emitted per nuclear transition, E_i = energy per radiation for the ith radiation (MeV). $\phi_i(T \leftarrow S)$ = fraction of energy emitted n a source region that is absorbed in a target region, m_T = mass of the target region (kg or g), and k = proportionality constant (Gy-kg/MBq-sec-MeV or rad-g/μCi-hr-MeV).

The proportionality constant k includes the various factors that are needed to obtain the dose rate in the desired units,

Department of Radiology and Radiological Sciences, Vanderbilt University, Nashville, TN.
Address reprint requests to Michael G. Stabin, PhD, CHP, Department of Radiology and Radiological Sciences, Vanderbilt University, 1161 21st Avenue South, Nashville, TN 37232-2675. E-mail: michael.g.stabin@vanderbilt.edu
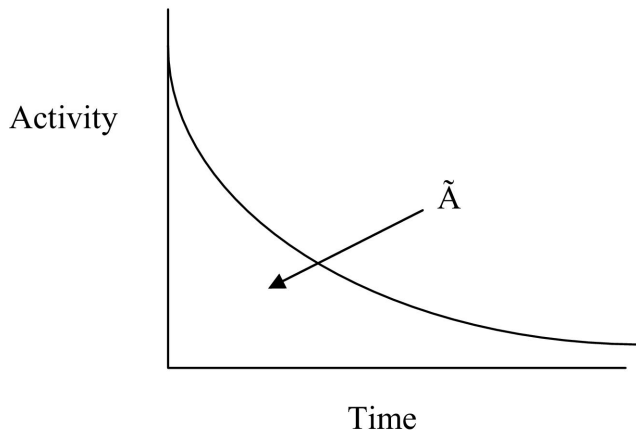
Figure 1 Generalized time–activity curve for an internal emitter.

from the units employed for the other variables, and it is essential that this factor is properly calculated and applied. Normally, this equation is integrated to provide estimates of absorbed dose, rather than dose rate. To calculate cumulative dose, the dose rate equation must be integrated. In most cases, the only term which depends on time is activity, so the only factor that has to be integrated is the activity term. The integral of the time-activity curve (ie, the area under that curve, regardless of its shape), gives the total number of disintegrations that have occurred over time in a source region (Fig. 1).

The equation for cumulative dose is:

$$D_T = \int \dot{D}_T \, dt = \frac{k \, \widetilde{A}_S \sum_i y_i \, E_i \, \phi_i(T \leftarrow S)}{m_T}$$

where D is the absorbed dose (Gy or rad) and The quantity $\widetilde{A}_S$ represents the integral of $A_S(t)$, the time-dependent activity within the source region:

$$\widetilde{A}_S = \int_0^\infty \widetilde{A}_S(t) \, dt = A_0 \int_0^\infty f_S(t) \, dt$$

where A_0 is the activity administered to the patient at time $t = 0$, and $f_S(t)$ may be called the fractional distribution function for a source region (fraction of administered activity present within the source region at time (t)). In many instances, the function $f_S(t)$ may be modeled as a sum of exponential functions:

$$f_S(t) = f_1 \, e^{-(\lambda_1 + \lambda_p)t} + f_2 \, e^{-(\lambda_2 + \lambda_p)t} + \; \cdots \; + f_N \, e^{-(\lambda_N + \lambda_p)t}$$

where terms $f_1 \ldots f_N$ represent the fractional uptake of the administered activity within the 1st to Nth compartments of the source region, $\lambda_1 \ldots \lambda_N$ represent the biological elimination constants for these same compartments, and λ_P represents the physical decay constant for the radionuclide of interest. Any functional expressions may be used to represent the time/activity behavior, but exponentials are most commonly encountered.

A generalized expression for calculating internal dose, which may describe the equations shown in publications by different authors (eg, MIRD,[3] RADAR,[4] ICRP[5]), can be calculated by the following equation:

$$D = N \times DF$$

where N is the number of nuclear transitions that occur in source region S (identical to $\widetilde{A}_S$), and DF is a "dose factor." The factor DF contains the various components shown in the formulas above, including terms describing the decay data, absorbed fractions, organ masses:

$$DF(T \leftarrow S) = \frac{k \sum_i y_i \, E_i \, \phi_i(T \leftarrow S)}{m_T}$$

The equations so far have resulted in the calculation of absorbed dose (Gy or rad); inclusion of radiation weighting factors, w_R, can take the calculation a step further to the estimation of equivalent dose (Sv or rem). Radiation weighting factors for some high linear energy transfer particles may not be equal to 1.0 in all cases; this subject will be discussed further herein.

$$DF(T \leftarrow S) = \frac{k \sum_i y_i \, E_i \, \phi_i(T \leftarrow S) w_{R_i}}{m_T}$$

As written, the aforementioned equations give only the dose from one source region to one target region, but they can be generalized easily to multiple source regions:

$$D_T = \frac{k \sum_S \widetilde{A}_S \sum_i y_i \, E_i \, \phi_i(T \leftarrow S) w_{R_i}}{m_T}$$

Basic Dose Calculational Methods: Anatomic Models and Computational Methods

The absorbed fractions defined in the last section are calculated through the use of anthropomorphic phantoms, mathematical models of the human body. The state of the art in this science for 3 decades was based on the Fisher–Snyder phantom,[6] which used a combination of geometric shapes, such as spheres, cylinders, cones, etc., to represent the human body in a way that allows Monte Carlo computer programs to simulate the creation and transport of photons through these various structures in the body. The mass of the organs and their atomic compositions and densities were based on data provided by the International Commission on Radiological Protection (ICRP) in its widely quoted definition of "Reference Man,"[7] which recently was updated in a more recent report.[8] These reports provide various anatomical data that are helpful in producing dose calculations for standardized individuals. Absorbed fractions and dose conversion factors (S values), as defined previously, for more than 100 radionuclides and more than 20 source and target regions, were published many years ago[9,10] but updated later and implemented in electronic tools for dose calculation.

Cristy and Eckerman[11] modified the adult male model and developed models for a series of individuals of different size and age (children of ages 0 [newborn], 1-year, 5-year, 10-year, and 15-year-olds, and adults of both genders). Ab-

sorbed fractions for photons at discrete energies were published for these phantoms, which contained approximately 25 source and target regions. Tables of S values (the MIRD name for *DF*) were never published but were made available to the user community in a personal computer code called "MIRDOSE,"[12] which was widely used by the nuclear medicine community, and was later updated to a Java-based personal computer code called OLINDA/EXM.[13] Stabin and coworkers developed a series of phantoms for the adult female, including a model of the nonpregnant adult female, and the woman at 3 stages of pregnancy.[14] These phantoms modeled the changes to the uterus, intestines, bladder, and other organs that occur during pregnancy and included specific models for the fetus, fetal soft tissue, fetal skeleton, and placenta. S values for these phantoms were also made available to the dosimetry community through the MIRDOSE and OLINDA/EXM software. Currently, these standardized models based on combinations of geometric constructs are being replaced with models based on medical image data that are far more realistic.[15] The realism of the newer models is shown in Figure 2, with comparison to the form of the existing models developed and implemented with stylized anthropomorphic models.

Models for Bone and Marrow

Spiers and colleagues[16] developed electron absorbed fractions for bone and marrow for an adult male subject; these results were used to calculate dose factors in MIRD Pamphlet No. 11.[7] Eckerman[17] re-evaluated this work and extended the results to derive dose factors for 15 skeletal regions in 6 models representing individuals of various ages. The results were also used in the MIRDOSE 3 software[12] to provide average marrow dose, regional marrow dose, and dose-volume histograms for different aged individuals. Bouchet and coworkers[18] used newer information on regional bone and marrow mass, and calculated new AFs using the EGS4 Monte Carlo code. Although the results of the Eckerman and Bouchet and coworkers models were similar in most characteristics and reported results, the models differed in a few important underlying assumptions. A revised model has been derived[19] which resolves these model differences in ways best supported by currently available data. New skeletal average absorbed fractions for all bone regions employed in the calculations in this study were implemented in the OLINDA/EXM[13] computer code. A number of investigations are also underway to employ image-based methods in producing more realistic bone and marrow dose models (eg, Shah and coworkers[20]); however, no functional model that can be used for dosimetry for subjects of different age and gender is available.

Quantification of Data for Use in Dose Assessment: Planar Imaging

Siegel and coworkers[21] defined basic methods for the gathering of adequate numbers of data points and of high-quality

Historical Adult Male Phantom	Realistic adult male model
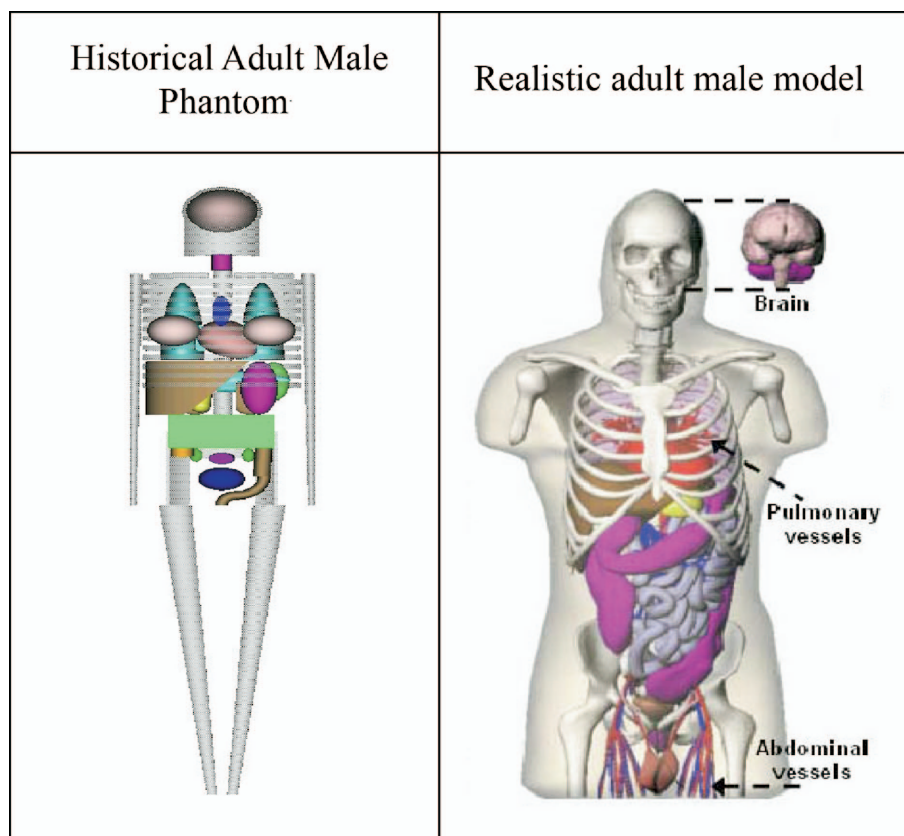
Figure 2 Comparison of the realism of the traditional body models with those being used to support current dose modeling efforts: Historical adult male phantom[6]; realistic adult male model.[15]

estimates of activity in source regions for dose assessment. Several quantification methods were discussed for planar imaging, as was the need to obtain 2 to 3 time points per phase of source region uptake or clearance to adequately characterize the kinetics. Accurate assessment of activity in organs, tumors, the rest of the body, and excretion are all necessary to completely characterize the kinetics, and thus dosimetry, of a given agent. Events representing energy deposition in nuclear medicine images must be converted to absolute values of activity (Bq or mCi), which requires that a calibration factor for the camera must be known, and that data are collected that permit correction of the raw images for radiation attenuation and scatter. In planar imaging, the external conjugate view counting pair (anterior/posterior) is the method most commonly used to obtain quantitative data for dosimetry. In this method, the source activity A_j is given by the expression:

$$A_j = \sqrt{\frac{I_A I_P}{e^{-\mu_e t}} \frac{f_j}{C}}$$

$$f_j \equiv \frac{(\mu_j t_j / 2)}{\sinh(\mu_j t_j / 2)}$$

where I_A and I_P are the observed counts in the anterior and posterior projections (counts/time), t is the overall patient thickness, μ_e is the effective linear attenuation coefficient, C is system calibration factor C (count rate per unit activity), and the factor f_j represents a correction for the source region attenuation coefficient (μ_j) and source thickness (t_j) (ie, source self-attenuation correction). This expression assumes that the views are well collimated (ie, they are oriented toward each other without offset). Corrections for scatter are usually necessary; a number of methods have been proposed. One relatively straightforward correction procedure for scatter compensation involves establishing adjacent windows on either side of the photopeak window, with the area of the 2 similar adjacent windows is equal to that of the photopeak.[22] The corrected (true) photopeak counts C_T are given by the expression:

$$C_T = C_{pp} - F_S * (C_{LS} + C_{US})$$

where C_{pp} is the total count recorded within the photopeak window, whereas C_{LS} and C_{US} are the counts within the lower and upper scatter windows, respectively. If the areas of the scatter windows are not equal (in sum) to that of the photopeak window, then an appropriate scaling factor (F_S) should be applied.

When a ROI is drawn over a source region on a projection image, some counts from the region will contain counts from activity in the subject's body that is outside of the identified source, including scattered radiation as discussed above, background radiation, and other sources. Background ROIs may be drawn over regions of the body that is close to the source ROI and which, in the investigator's best judgment, best represents the underlying tissue in which the source resides and which will provide the best estimate of a background count rate to be subtracted from the source ROI. Background ROIs should not be drawn over a major blood vessel or other body structure that contains a high level of activity, as this will remove too many counts from the source ROI. The choosing of locations and sizes of background ROIs is very difficult to prescribe exactly, and methods between investigators differ, possibly resulting in markedly different results for the final estimates of activity assigned to a source ROI.

Source organ regions may also have problems with overlapping regions on projection images. The right kidney and liver are frequently partially superimposed on such images, as are the left kidney and spleen, for example. When organ overlap occurs, an estimate of the total activity within a source can be obtained by a number of approximate methods. For paired organs, such as kidneys and lungs, one approach is to simply quantify the activity in one of the organs for which there is no overlap with other organs and multiply the number of counts in this organ by 2 to obtain the total counts in both organs. Another approach is to draw a ROI over the organ region in scans where there is overlap, count the number of pixels and note the average count rate per pixel, then use a ROI from another image in which there is no apparent overlap and the whole organ is clearly visible, count the number of pixels in a larger ROI drawn on this image, and then multiply the count rate per pixel from the first image by the number of pixels in the second image. Or, equivalently, take the total number of counts in the first image and multiply by the ratio of the number of pixels in the second to the first image ROIs. If no image can be found in which a significant overlap with another organ does not obscure the organ boundaries, an approximate ROI may need to be drawn just from knowledge of the typical shapes of such organs. This kind of approximation is obviously not ideal, but may be a necessary approximation. Another approach is the use of lateral view projection images, which may be helpful in resolving some overlap issues.

Calibration and attenuation coefficients for each radionuclide and gamma camera/collimator combination are obtained by imaging a small source of known activity for a fixed amount of time. The attenuation coefficient for a given camera may be estimated by imaging this source with various known thicknesses of tissue-equivalent material interposed between the source and camera and fitting the results to an exponential function.

Quantification of Data for Use in Dose Assessment: Use of Tomographic Data

Data from tomographic imaging are in general superior to those from planar images because problems of overlap may be resolved, increased contrast between regions may be obtained, and more accurate information about activity (and thus dose) distribution may be obtained. Tomographic data are particularly helpful in evaluating heterogeneous uptakes of activity in source organs or and resolving issues of underlying or overlying background activity. Data collected with positron emission tomography (PET) imaging may provide

data for PET agents; standardized uptake values (SUVs) are used to quantify radiotracer uptake at some time of measurement:

$$SUV = \frac{\text{tracer activity concentration in tissue}}{\text{injected tracer activity/patient weight}}$$

Quantification of data with single-photon emission computed tomography (SPECT) methods data are also applied to dosimetry calculations. Standard software on all commercial systems provides well-established methods for scatter and attenuation corrections. Methods for SPECT image reconstruction and quantification are under constant revision, and new advances promise improved results that will be helpful in dose assessment.[23-25] These authors discuss some of the complex issues important to perform good SPECT quantification, including basic calibration, attenuation and scatter correction, and corrections for dead time and partial volume effects.

Current Practice: Diagnostic Agents

Dose calculations for diagnostic agents are calculated with animal or human (healthy volunteers or patients) data during the initial drug approval process. Animal data may be extrapolated by a variety of methods, none of which is necessarily standard.[26] Human data are most often analyzed using the conjugate-view approach described above, although PET imaging may be used to obtain quantitative data for positron emitting agents (eg, see Sgouros et al[27]). Dosimetry for these agents, given for average adults and children[28,29] using the standard body models described previously are usually accepted as adequate for basic risk/benefit analyses.

Current Practice: Therapeutic Agents

Imaging of patients to obtain anatomical and physiological information has progressed substantially in recent years. Anatomic information obtained from medical images, obtained with magnetic resonance imaging (MRI) or computed tomography (CT) approaches, can be expressed in 3 dimensions (3D) in voxel format, with typical resolutions on the order of 1 mm. Similarly, SPECT and PET imaging systems can provide 3D representation of patient-specific activity distributions, with typical resolutions of around 5 to 10 mm. Many imaging systems now combine CT with PET or SPECT imaging systems on the same imaging gantry, so that patient anatomy and tracer distribution can be imaged during a single session without moving the patient, thus facilitating image registration. Monte Carlo radiation transport codes may then be used to perform patient-specific 3D dose calculations. Such effort is not needed for the routine use of diagnostic agents; careful, patient-specific optimization is generally not performed for nuclear medicine therapy patients, either, as is routinely done in radiation therapy using external sources of radiation (radiation producing machines, brachytherapy). Physicians generally have low confidence in the use of these radiation dose analyses to plan individual subject therapy, partially because of limitations on the accuracy of activity quantification and also due to the lack of realism in current body models used for dose assessment. Thus, a "one-dose-fits-all" approach to therapy is usually used, with conservatism generally resulting in administration of lower than optimum levels of activity to the majority of subjects, to the detriment of patient care. The use of imaging data, as described previously, has been used to develop new realistic reference phantoms, as well as to facilitate patient-specific models for individual therapy patients. Examples of use of patient-individualized, image-based dosimetry modeling will be given herein.

Patient-Individualized Adjustment of Calculated Dose

Fairly simple modifications can be made to the standard equations shown previously in cases in which the mass of an individual's organ is known to be significantly different than that of the standardized phantom used. For alpha and beta emissions, a linear scaling of dose with mass is appropriate, as the absorbed fraction for emissions when the source is the target is just 1.0, and thus the DF just changes inversely with changes in mass of the organ. That is:

$$DF_2 = DF_1 \frac{m_1}{m_2}$$

Here, DF_1 and DF_2 are the dose factors appropriate for use with organ masses m_1 and m_2. For photons, Snyder[30] showed that the photon absorbed fractions vary directly with the cube root of the mass for self-irradiation (ie, source = target) if the photon mean path length is large compared with the organ diameter, and vary directly with the mass for cross-irradiation (ie, source ≠ target). What the latter point shows is that the specific absorbed fraction for cross-irradiation does not change with differences in mass, provided the source and target are sufficiently separated and that the change in mass of one or both does not appreciably change the distance between them. Thus, for self-irradiation, the absorbed fraction increases with the cube root of the mass of the organ, and thus the specific absorbed fraction decreases with the two-thirds power of the mass[31]:

$$\phi_2 = \phi_1 \left(\frac{m_2}{m_1}\right)^{1/3} \qquad \Phi_2 = \Phi_1 \left(\frac{m_1}{m_2}\right)^{2/3}$$

This relationship is useful, but not necessarily exactly true for all body regions and radionuclides.[32]

Traino and colleagues showed how to perform modifications to the standard dose equations to account for changes in thyroid mass as a function of time during ^{131}I thyroid therapy.[33] If the thyroid final mass, m_{fin}, can be related to the initial mass, m_0 and delivered dose D_T as follows:

$$m_{fin} = m_0 \exp(-\alpha D_T)$$

then the administered activity for a subject can be calculated as:

$$A_0 = \frac{2 \ln(2) \, m_0}{\Delta_{np} \, U \, \alpha[\ln(2) \, T_{max} + 2T_{eff}]} \ln\left(\frac{m_{fin}}{m_0}\right)$$

Similarly, changes in lesion mass during therapy and the effect on dose calculations have been studied by Hindorf and coworkers[31] and Harman Siantar and coworkers[34] Traino and coworkers also showed how to scale red marrow dose factors for patient size[35] (see Traino et al[35] for definitions of the terms):

$$D_{RM} = [A_{bl}] \times m_{RM}\frac{m_{tb}}{m_{TB}} \times RMBLR \times S_{RM \leftarrow RM} \times \left(\frac{m_{TB}}{m_{tb}}\right)$$

$$+ \left(\widetilde{A}_{tb} - [A_{bl}] \times m_{RM}\frac{m_{tb}}{m_{TB}} \times RMBLR\right)$$

$$\times \left[S_{RM \leftarrow TB} \times \left(\frac{m^2_{TB}}{m_{tb} \, m_{RB}}\right)^{x_1}\left(\frac{m_{TB}}{m_{tb}}\right)^{x_2}\right.$$

$$\left. - S_{RM \leftarrow RM} \times \left(\frac{m_{RM} \, m^2_{TB}}{m^2_{tb} \, m_{RB}}\right)\right]$$

Standard Dose Estimates for Radiopharmaceuticals

The approaches and models described previously may be used by many individuals and groups to calculate dose estimates for different radiopharmaceuticals. It can sometimes be frustrating to some users to seek dosimetry information on a particular radiopharmaceutical and find several different sets of dose estimates, often with minor and sometimes significant discrepancies in the models employed and the resulting doses calculated. Standardized dose calculations for a few radiopharmaceuticals (less than 20) were developed by the MIRD Committee during a 30-year period. Estimates for more than 80 radiopharmaceuticals were published in 1996 by the dosimetry information center in Oak Ridge.[36] Most recently, compendium of dose estimates for about 200 radiopharmaceuticals has been published by a working group of the ICRP, based on the best known biodistribution data and using the standard models described above.[37] These values are referenced in most cases in which standardized dose estimates for a particular radiopharmaceutical are needed.

Image-Based Computational Tools

A number of centers are experimenting with the idea of using image fusion techniques to develop 3-dimensional maps of dose, instead of only average organ dose estimates from standard models. This represents a generational change in dose models and points to a new era in radionuclide dosimetry in which sophisticated dosimetry treatment planning for internal emitters may be similar to that used in external beam therapy for individualized patient therapy planning. Exam-

ples include the 3D-ID code from the Memorial Sloan-Kettering Cancer Center,[38] the SIMDOS code from the University of Lund,[39] the RTDS code at the City of Hope Medical Center,[40] the RMDP code from the Royal Marsden Hospital,[41] and the DOSE3D code.[42] The code with the most clinical experience to date is the 3D-ID code; Figure 3 shows an example of the capabilities of this code. These codes either rely on the standard geometrical phantoms (MABDose and DOSE3D) or patient-specific voxel phantom data (3DID and SIMDOS) and various in-house written routines to perform photon transport. Neither has a particularly robust and well supported electron transport code, such as is available in EGS,[43] MCNP,[44] or GEANT.[45] The PEREGRINE code[46] has also been proposed for 3-dimensional, computational dosimetry and treatment planning in radioimmunotherapy.[47]

Correlation of Calculated Dose With Effect

Attempts to correlate hematological toxicity with marrow dose, when marrow cells are specifically targeted, have not been particularly successful in the past, in part as the result of uncertainties in the actual absorbed dose, but also because of the difficulty in assessing marrow functional status before therapy.[48-55] Correlations of a number of marrow toxicity indices with marrow dose for ^{90}Y-labeled Zevalin, calculated with the reference adult phantom using the MIRDOSE[12] code, on more than 150 subjects, were disappointing.[56] This led to the approval of the compound with no requirement for performing patient-individualized dose calculations. It is clear that 1-dimensional dose calculations with standard, reference subjects will not produce dose calculations that will be of sufficiently high quality to be used in therapy planning. Characterization of patient-specific organ mass and body anatomy must accompany the characterization of tumor and normal tissue uptake and retention. Realistic, rather than "stylized" body morphometry, based on patient images (from CT, for instance) are now possible on a patient-individualized basis and must form the basis for calculations in therapy.

Several investigators have shown recently that patient-specific dose calculations can indeed produce strong correlations between calculated dose and observed effects in tumors and normal tissues. The methods shown by these investigators should be widely adopted and used by others as dose calculations in nuclear medicine therapy become a routine part of providing patients with the best possible therapy and therefore the best possible and durable responses to their therapy. Shen and coworkers,[57] using a ^{90}Y-antibody in radioimmunotherapy, obtained an r value of 0.85 for correlation of marrow dose with observed marrow toxicity, using patient-specific marrow mass estimated from CT images and estimation of the total marrow mass from the mass of the marrow in 3 lumbar vertebrae. Siegel and coworkers[58] obtained a correlation coefficient of 0.86 between platelet nadir and calculated marrow dose but with an ingenious modification based on the levels of a stimulatory cytokine (FLT3-L) measurable in peripheral blood that reflects the functional
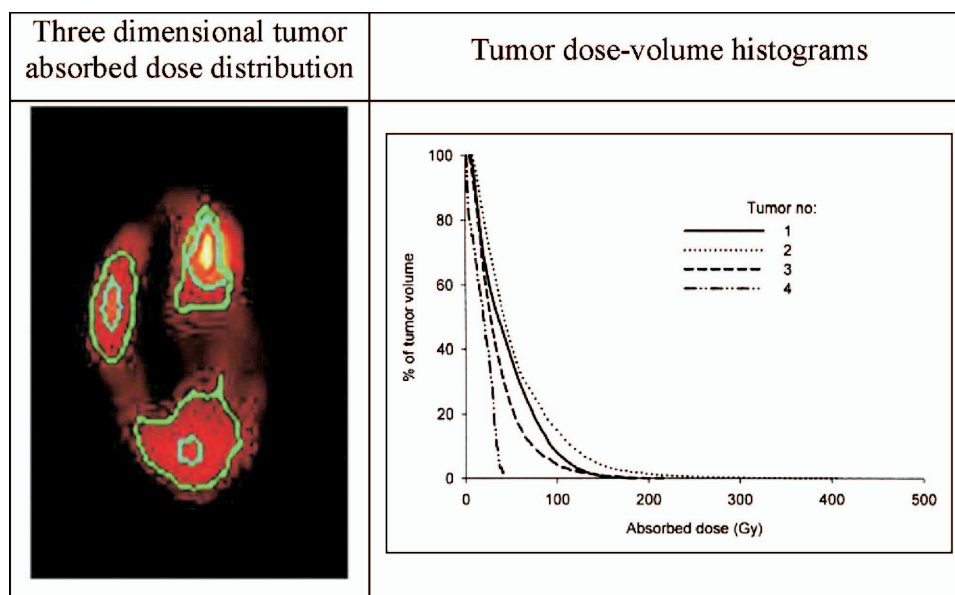
Figure 3 Three-dimensional tumor absorbed dose distributions (left) and dose-volume histograms (right) calculated with the 3D-ID code.[47] Three-dimensional tumor absorbed dose distribution. Tumor dose-volume histograms.

status of a subject's marrow, in a study using an ^{131}I anti-cea antibody. Although others have failed to find firm correlations between tumor dose and observed response, Pauwels and coworkers found a convincing relationship, in their study of 22 patients with [90]Y Octreother.[59] Kobe and coworkers[60] evaluated the success of treatment of Graves' disease in 571 subjects, with the goal of delivering 250 Gy to the thyroid, with the endpoint measure being the elimination of hyperthyroidism, evaluated 12 months after the treatment. Relief from hyperthyroidism was achieved in 96% of patients who received more than 200 Gy, even for thyroid volumes >40 mL. Individually tailored patient thyroid dosimetry was made to the targeted total dose, with ultrasound measurement of subject thyroid mass and adjustment of the procedure to account for differences between observed effective retention half-times between studies involving the tracer activity and the therapy administration. These authors note that success rates with more traditional treatments (not using individually tailored dosimetry) are typically at best 60% to 80%.

Two clinical considerations that are difficult to quantify are also of importance in the management of individual patients. Large variations in thyroid radiosensitivity exist between individuals. There is a strong correlation between the amount of activity administered and the rate and timing of euthyroid response and subsequent hypothyroid induction. Practical clinical considerations are taken into account when determining the amount of activity to be administered to a particular patient. For example, a severely hyperthyroid patient may be administered more activity than the dose formula would dictate than a less toxic patient if speed of remission is important because of the patient's medical condition. The increased incidence of subsequent hypothyroidism would be an accepted manageable consequence. A less severely ill patient who is likely to be lost to clinical follow-up may receive less than the formula driven amount to decrease the likelihood of subsequent untreated hypothyroidism the consequence of which loom large. There is a well documented strong correlation between the amount of ^{131}I administered[61] and the μCi/g deposited in the gland[62] and the incidence of hypothyroidism.

Furthermore, some evidence is indicating that the biologically effective dose (BED), not just the absorbed dose, is the parameter that should be characterized, in both internal and external dose calculations.[63-65] The fraction of cells surviving an irradiation (SF) as a function of the dose delivered (D) is often represented as:

$$\ln(SF) = -\alpha D - \beta D^2$$

where α and β are parameters related to tissue radiosensitivity; the ratio of these parameters determine the shape of a cell survival curve (Fig. 4). Generally the term α is thought to describe cell death from single hits, whereas the β term has dose rate dependence. It is therefore thought that the β term is of greater importance in targeted radionuclide therapy (TRT).[66] A dose protraction factor, G, has been added to this
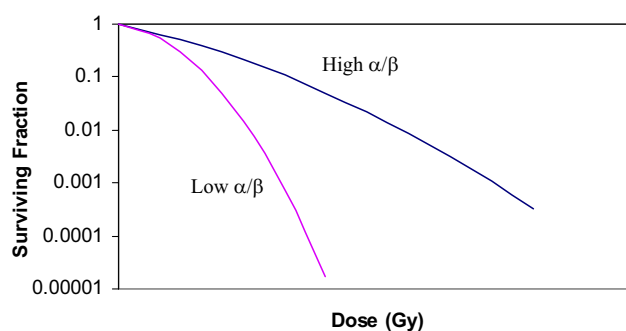
Figure 4 Cell survival curves and relation to the α/β ratio.

model[67,68] to accommodate the effect on cell killing of dose rate:

$$G = \frac{2}{D^2} \int\limits_0^\infty \dot{D}(t) \int\limits_0^t \dot{D}(t') e^{-\mu(t-t')} dt' dt$$

Here, μ is a constant describing sublethal damage repair and t' is a time-point during therapy before time t.

BED was introduced to provide a practical implementation of these ideas[69,70]:

$$BED = \frac{\ln(SF)}{\alpha}$$

This model has been used to compare absorbed doses delivered with TRT with those delivered with external beam radiotherapy using the following equations:

For external beam radiotherapy:

$$BED_{EBT} = D_{EBT} \left(1 + \frac{D_{EBT}/n}{\alpha/\beta} \right)$$

and for TRT:

$$BED_{TRT} = D_{TRT} \left(1 + \frac{D_{TRT}\lambda}{(\mu + \lambda)(\alpha/\beta)} \right)$$

TRT is frequently used to treat patients with a wider variation in disease progression and treatment background. Important implications exist regarding the heterogeneity of uptake of radiopharmaceuticals,[71] so the application of radiobiological concepts are arguably of greater relevance than is the case for external beam radiotherapy. This area of research remains an active one.[72] The application of the BED approach in patient-individualized, image-based 3D dosimetry is under investigation.[73] It is possible that radiobiological arguments may be employed to combine TRT and external beam radiotherapy.[74]

Other Biological Variables

Recent experimental evidence has shown that energy distribution alone cannot always predict the occurrence of cellular changes but that, in some conditions, cells with no direct energy deposition from radiation may demonstrate a response (the "bystander effect"). Brooks notes that "The potential for bystander effects may impact risk from nonuniform distribution of dose or energy in tissues and raises some very interesting questions as to the validity of such calculations." Hall[75] notes that "The plethora of data now available concerning the bystander effect fall into two quite separate categories, and it is not certain that the two groups of experiments are addressing the same phenomenon." Those two categories are medium transfer experiments, and microbeam irradiation experiments. Other striking studies have involved the irradiation of the lung base in rats, with a marked increase in the frequency of micronuclei found in the shielded lung apex.[76] However, radiation of the lung apex did not result in an increase in the chromosome damage in the shielded lung base. This suggests that a factor was transferred from the exposed portion of the lung to the shielded part and that this transfer has direction from the base to the apex of the lung. In another experiment, exposure of the left lung resulted in a marked increase in micronuclei in the unexposed right lung. Experiments suggest that bystander effects are limited to the organ irradiated, and have been demonstrated primarily in experiments with alpha particles. These results challenge the traditional notion of the relationship of dose and effects. Sgouros and coworkers[77] recently provided an overview of this area and its possible impact on dosimetry in nuclear medicine.

Clinical Experience With Dosimetry

Clinical applications of dosimetry to TRT are of general interest but are not widely performed, mainly because of the lack of data from comprehensive clinical trials that may prove the effectiveness of dosimetry in predicting therapy outcomes. A lack of standardized methodology leads to significant difficulty in comparisons of results between trials.[78] The continued use of approaches based on uniform activity administrations to all patients without evaluation of radiation dose has hampered efforts to understand how radiation dose relates to effects and outcomes in patient populations. More widespread acceptance of standardized dose calculational techniques is needed to advance this science.

Diseases of the Thyroid

There has been significant debate about the use of dosimetry in the evaluation and treatment of benign thyroid disease. A number of authors advocate patient-specific determination of administered activities to deliver a prescribed absorbed dose, but the majority of practice is still based on fixed activity approaches. Uptake of radioiodine varies widely from patient to patient, and more notably for subjects with autonomous nodules than for those with primarily normal tissue.[79] The use of ^{124}I NaI PET to perform tracer dosimetry has been shown to produce absorbed dose estimates with an accuracy of within 10%.[62] It has been shown that an absorbed therapeutic dose can be predicted by a prior tracer administration to within a degree of accuracy that would enable patient-specific treatment planning[80,81] and it has further been shown that the rate of hypothyroidism resulting from the treatment of Graves disease with radioiodine is correlated with the absorbed dose.[62,82,83]

Treatment of thyroid cancer with ^{131}I NaI is the most common oncological application of TRT and has been used for many decades. There have been few changes in treatment regimens in that time, but there is also no internationally agreed on method for treatment. In the majority of cases, treatments are based on fixed activities rather than absorbed doses, although there are some exceptions.[84,85] Typically, patients will are given between 1 and 3 GBq for ablation and 3 and 20 GBq for subsequent therapies.[86] Benua and coworkers[87] described a patient-specific approach to choosing administered activity based on whole-body dose. Other authors have suggested the use of ^{124}I NaI to facilitate dosimetry for the treatment of thyroid cancer.[88,89] Where dosimetry has

been performed, it is clear that a wide range of tumor absorbed doses may be delivered from fixed activities, as subjects have significantly different iodine uptakes and clearance half-times.[53,90] However, because of the simplicity of the treatment method, the lack of complications, and widespread use, radioiodine treatment of thyroid cancer should be able to provide abundant data for evaluating dose-response criteria that could lead to a confident patient-specific treatment approach.[91] The issue of thyroid stunning is a complication; there is still doubt as to the level of activity or dose above which stunning occurs. This phenomena is perhaps less relevant for ^{123}I or [124]I, and stunning from ^{131}I is known to be an early therapeutic effect.[92-94] Other complications involved with ^{131}I therapy include salivary gland dysfunction and pain, transient depression of bone marrow and reduced fertility in some cases.[95] Some have investigated long term risks of leukemia and other malignancies, but follow-up studies do not show a reproducible occurrence, thus the risk is probably small if present.[96]

[131]I mIBG Therapy

[131]I meta-iodobenzylguanidine (mIBG) has been used for many years for the treatment of adult and pediatric neuroendocrine tumors, including pheochromocytoma, paraganglioma, and neuroblastoma. Administration protocols vary widely from standard administrations of approximately 7.4 GBq to activities greater than 30 GBq (in adults).[97-99] As with radioiodine treatment of thyroid cancer, the number and frequency of administrations also varies widely from site to site. Current problems with this therapy that could be addressed with dosimetry include the issue of carrier-added mIBG; currently only a small fraction of the mIBG that is infused is labeled with [131]I. Where dosimetry has been evaluated, it has been shown that a wide variation in absorbed doses to either the whole-body and to tumor and normal organs will result from a fixed administered activity approach.[60,100,101] A multicenter clinical trial involving dosimetry treating relapsed or refractory neuroblastoma has recently been started in Europe. This study uses a criterion of a whole-body absorbed dose of 4 Gy in 2 fractions.[98]

Radioimmunotherapy

The use of monoclonal antibodies for has been of interest for cancer treatment for many decades. Clinical research has led to the develppment of 2 important products against non-Hodgkin's lymphoma, ^{131}I-labeled Bexxar and ^{90}Y-labeled Zevalin. These 2 products, which use an anti-CD20 antibody, have been approved by the U.S. Food and Drug Administration for the treatment of relapsed or refractory B-cell non-Hodgkin's lymphoma. The clinical efficacies of these treatments have not been directly compared in a trial, but both demonstrated superior clinical efficacy to nonradioactive products during their drug approval process. Sales of the drugs have been disappointing to date, as the result of various factors, and the future of their use at present is in doubt.[102] Zevalin is administered with no dosimetry regimen at all,[103] for reasons discussed herein, treatment with Bexxar is based

on limiting whole-body dose (as a surrogate for marrow dose) to 0.75 Gy.[104]

Radiopeptide Therapy

Peptide therapy for neuroendocrine tumors has shown success in the form of somatostatin analogues such as DOTA-DPhe(1)-Tyr(3)-octreotide (DOTATOC), with several dosimetric studies presented.[105] A study by Hindorf and coworkers[106] found that tumor absorbed doses resulting from a fixed administration of ^{90}Y DOTATOC varied widely on an interpatient basis, although in repeated treatments the intrapatient variation was much smaller, indicating that it would be possible in principle to use dosimetric results from the first therapy to adjust subsequent therapies. Barone and coworkers[107] calculated kidney absorbed dose from administrations of ^{90}Y DOTATOC. They evaluated the BED and found a strong correlation between BED and creatinine clearance. Studies are ongoing to compare the relative efficacies of DOTATOC with DOTATATE and the best radionuclide to use with either.[108] A major problem with peptide-based radiotherapy is the large dose to the kidney, and extensive investigations are ongoing to block receptors, add radiation protection agents/procedures, and/or modify transit time.[109]

Summary of Clinical Experience

The clinical introduction of internal dosimetry for TRT has been slow and is still far from being implemented routinely, even in Europe, where a European directive stating that 'For all medical exposure of individuals for radiotherapeutic purposes, including nuclear medicine for therapeutic purposes, exposures of target volumes shall be individually planned; taking into account that doses of nontarget volumes and tissues shall be as low as reasonably achievable and consistent with the intended radiotherapeutic purpose of the exposure (EURATOM 97/43[110]). In cases in which dosimetry is performed, the methodology used generally is adapted from radiation protection rather than radiotherapy principles. Recent studies have shown conclusively that the administration of fixed activities results in a wide range of absorbed doses and there is now initial evidence to suggest that patient outcome is more likely to be correlated with absorbed dose rather than administered activity. It is vital for patients' interests that dose assessment for tumor and for normal tissues become routine in clinical practice, aided by improved techniques and a significant improvement in our understanding of radiobiological considerations.

The Need for Patient-Individualized Optimization of Therapy

Although it is well known that patients vary substantially in tumor and normal organ radiopharmaceutical uptake and clearance half-times, physicians continue to administer similar levels of activity or activity per unit total body mass to all patients with no dosimetric analysis.[111] This is well tolerated in the use of radioiodines against thyroid cancer and hyperthyroidism, as the "therapeutic window" (difference in dose

levels between what is experienced by the tumor and that experienced by the most important normal tissue) is large. Nonetheless, optimizing patients' therapy in this application is desirable to minimize the risk of unwanted side effects such as sialadenitis and sicca syndrome,[112] and is clearly in the patients' best interests (in avoiding frequent retreatment) and in the treating institution's best interests (economically), as shown by Kobe and coworkers,[60] and discussed above. In other, recently evolving forms of therapy (eg, the use of monoclonal antibodies for and radiolabeled peptides in therapy), the tumor-to-normal tissue absorbed dose ratio may be low, and without the use of a patient-specific treatment planning strategy based on dose assessment, we know that patients are frequently treated cautiously and most are given low amounts of the therapeutic agent, to avoid deleterious effects in normal tissues (most notably the bone marrow). Different patients will have different levels of tumor and normal tissue uptake concentrations, as well as in the clearance rates at which activity leaves these tissues. Patients who clear the activity more slowly from their bodies will necessarily receive higher doses to marrow and other normal tissues than those with faster rates of elimination. Thus only some patients will receive optimal care, and a majority of patients will receive a lower than optimal administration of activity. This usually results in no deleterious effects in normal tissues, but suboptimal therapy being delivered to the malignant tissues, with poor response rates and high rates of relapse. As was stated by Siegel and coworkers[113]:

> If one were to approach the radiation oncologist or medical physicist in an external beam therapy program and suggest that all patients with a certain type of cancer should receive the exact same protocol (beam type, energy, beam exposure time, geometry, etc.), the idea would certainly be rejected as not being in the best interests of the patient. Instead, a patient-specific treatment plan would be implemented in which treatment times are varied to deliver the same radiation dose to all patients. Patient-specific calculations of doses delivered to tumors and normal tissues have been routine in external beam radiotherapy and brachytherapy for decades. The routine use of a fixed GBq/kg, GBq/m², or simply GBq, administration of radionuclides for therapy is equivalent to treating all patients in external beam radiotherapy with the same protocol. Varying the treatment time to result in equal absorbed dose for external beam radiotherapy is equivalent to accounting for the known variation in patients' uptake and retention half-time of activity of radionuclides to achieve equal tumor absorbed dose for internal-emitter radiotherapy. It has been suggested that fixed activity-administration protocol designs provide little useful information about the variability among patients relative to the normal organ dose than can be tolerated without dose-limiting toxicity compared with radiation dose-driven protocols.

Thierens and coworkers[114] noted that ". . . patient-specific dose calculations in radionuclide therapy are difficult to perform and possibly subject to large error. Therefore, individual dosimetry-based activity calculations are not routinely applied yet and a large variety of methodologies exists for determining the administered activity in clinical practice. . . ." They also noted, however, that ". . . as absorbed dose estimates become more patient-specific, an improved correlation between the administered activity and the clinical outcome may be expected. It is clear that a patient-specific treatment planning will improve the quality of radionuclide therapy substantially, especially in a curative setting."

The idea of patient-individualized dosimetry for nuclear medicine patients remains controversial. Many feel that it is essential that in *all* forms of radiotherapy with internal emitters, a patient-individualized dose calculation be made when possible for the most important tumors for which a specific uptake of the radiopharmaceutical can be made, and for the most important normal tissue at risk (generally the bone marrow, but possibly the lungs, kidneys, or other organs). Others argue that clear data showing an improvement in efficacy and outcome have not yet been realized.[115] Dosimetry is needed not only to provide a better quality of therapy to patients treated currently, but also to establish a database of literature that can be used to understand the variability between subjects and the range of uptake and clearance values to be expected for different therapy agents. Standardized methods for calculating dose are well established and automated at present, and should be used to provide dose calculations that are comparable and reproducible between institutions.

References

1. Marinelli L, Quimby E, Hine G: Dosage determination with radioactive isotopes II, practical considerations in therapy and protection. Am J Roent Radium Ther 59:260-280, 1948
2. Quimby E, Feitelberg S: Radioactive Isotopes in Medicine and Biology. Philadelphia, Lea and Febiger, 1963
3. Loevinger R, Budinger T, Watson E: MIRD Primer for Absorbed Dose Calculations. Reston, VA, Society of Nuclear Medicine, 1988
4. Stabin MG, Siegel JA: Physical models and dose factors for use in internal dose assessment. Health Phys 85:294-310, 2003
5. International Commission on Radiological Protection: 1990 Recommendations of the International Commission on Radiological Protection. ICRP Publication 60. New York, Pergamon Press, 1991
6. Snyder W, Ford M, Warner G, et al: MIRD Pamphlet No 5 - Estimates of Absorbed Fractions for Monoenergetic Photon Sources Uniformly Distributed in Various Organs of a Heterogeneous Phantom. J Nucl Med Suppl 3:5, 1969
7. International Commission on Radiological Protection: ICRP Publication 23, Task Group Report on Reference Man. Oxford, Pergamon Press, 1975
8. International Commission on Radiological Protection: ICRP Publication 89: Basic Anatomical and Physiological Data for Use in Radiological Protection: Reference Values. New York, Elsevier Health, 2003
9. Snyder W, Ford M, Warner G: Estimates of specific absorbed fractions for photon sources uniformly distributed in various organs of a heterogeneous phantom. MIRD Pamphlet No. 5, revised. New York, Society of Nuclear Medicine, 1978
10. Snyder W, Ford M, Warner G, et al: A Tabulation of Dose Equivalent Per Microcurie-Day for Source and Target Organs of an Adult for Various Radionuclides. ORNL-5000. Oak Ridge, TN: Oak Ridge National Laboratory, 1975
11. Cristy M, Eckerman K: Specific Absorbed Fractions of Energy at Various Ages From Internal Photons Sources. ORNL/TM-8381 V1-V7. Oak Ridge, TN: Oak Ridge National Laboratory, 1987

12. Stabin M: MIRDOSE: The personal computer software for use in internal dose assessment in nuclear medicine. J Nucl Med 37:538-546, 1996

13. Stabin MG, Sparks RB, Crowe E: OLINDA/EXM: The second-generation personal computer software for internal dose assessment in nuclear medicine. J Nucl Med 46:1023-1027, 2005

14. Stabin M, Watson E, Cristy M, et al: Mathematical models and specific absorbed fractions of photon energy in the nonpregnant adult female and at the end of each trimester of pregnancy. ORNL Report ORNL/TM-12907, 1995

15. Segars JP: Development and Application of the New Dynamic NURBS-based Cardiac-Torso (NCAT) Phantom, PhD Dissertation, The University of North Carolina, 2001

16. Spiers FW: Beta dosimetry in trabecular bone, in Mays CW (ed): Delayed Effects of Bone-Seeking Radionuclides. Salt Lake City, UT, University of Utah Press, 1969, pp 95-108

17. Eckerman K, Stabin M: Electron absorbed fractions and dose conversion factors for marrow and bone by skeletal regions. Health Phys 78:199-214, 2000

18. Bouchet LG, Bolch WE, Howell RW, et al: S-Values for radionuclides localized within the skeleton. J Nucl Med 41:189-212, 2000

19. Stabin MG, Eckerman KF, Bolch WE, et al: Evolution and status of bone and marrow dose models. Cancer Biother Radiopharm 17:427-434, 2002

20. Shah AP, Bolch WE, Rajon DA, et al: A paired-image radiation transport model for skeletal dosimetry. J Nucl Med 46:344-353, 2005

21. Siegel J, Thomas S, Stubbs J, et al: MIRD Pamphlet No 16—Techniques for Quantitative Radiopharmaceutical Biodistribution Data Acquisition and Analysis for Use in Human Radiation Dose Estimates. J Nucl Med 40:37S-61S, 1999

22. Ogawa K, Harata Y, Ichihara T, et al: A practical method for position-dependent Compton-scatter correction in single emission CT. IEEE Trans Medimag 10:408-412, 1991

23. King M, Farncombe T: An overview of attenuation and scatter correction of planar and SPECT data for dosimetry studies. Cancer Biother Radiopharm 18:181-190, 2003

24. Autret D, Bitar A, Ferrer L, et al: Monte Carlo modeling of gamma cameras for I-131 imaging in targeted radiotherapy. Cancer Biother Radiopharm 20:77-84, 2005

25. Dewaraja YK, Wilderman SJ, Ljungberg M, et al: Accurate dosimetry in I-131 radionuclide therapy using patient- specific, 3-dimensional methods for SPECT reconstruction and absorbed dose calculation. J Nucl Med 46:840-849, 2005

26. Kirschner A, Ice R, Beierwaltes W: Radiation dosimetry of [131]I-19-iodocholesterol: The pitfalls of using tissue concentration data, the author's reply. J Nucl Med 16:248-249, 1975

27. Sgouros G, Kolbert KS, Sheikh A, et al: Patient-specific dosimetry for ^{131}I thyroid cancer therapy using 124I PET and 3-dimensional-internal dosimetry (3D-ID) software. J Nucl Med 45:1366-1372, 2004

28. International Commission on Radiological Protection: ICRP Publication 53: Radiation Dose to Patients from Radiopharmaceuticals, 53. New York, Pergamon, 1989

29. International Commission on Radiological Protection: Radiation Dose to Patients from Radiopharmaceuticals. ICRP Publication 80, New York, Pergamon, 2000

30. Snyder W: Estimates of absorbed fraction of energy from photon sources in body organs. Medical Radionuclides: Radiation Dose and Effects, USAEC, 1970, pp 33-50

31. Hindorf C, Linden O, Stenberg L, et al: Change in tumor absorbed dose due to decrease in mass during fractionated radioimmunotherapy in lymphoma patients. Clin Cancer Res 9:4003s-4006s, 2003

32. Siegel JA, Stabin MG: Mass-scaling of S Values for blood-based estimation of red marrow absorbed dose: The quest for an appropriate method. J Nucl Med 48:253-256, 2007

33. Traino AC, Di Martino FA: Dosimetric algorithm for patient-specific 131I therapy of thyroid cancer based on a prescribed target-mass reduction. Phys Med Biol 51:6449-6456, 2006

34. Hartman Siantar CL: Impact of nodal regression on radiation dose for

35. Traino AC, Ferrari M, Cremonesi M, et al: Influence of total-body mass on the scaling of S-factors for patient-specific, blood-based red-marrow dosimetry. Phys Med Biol 52:5231-5248, 2007

36. Stabin MG, Stubbs JB, Toohey RE: Radiation Dose Estimates for Radiopharmaceuticals. NUREG/CR-6345, prepared for: US Nuclear Regulatory Commission, US Department of Energy, US Department of Health & Human Services, 81 pages, 1996

37. International Commission on Radiological Protection: Radiation Dose Estimates for Radiopharmaceuticals. ICRP Publications 53 and 80, with addenda. New York, Pergamon Press, 1983-1991

38. Kolbert KS, Sgouros G, Scott AM, et al: Implementation and evaluation of patient-specific three-dimensional internal dosimetry. J Nucl Med 38:301-308, 1997

39. Dewaraja YK, Wilderman SJ, Ljungberg M, et al: Accurate dosimetry in 131I radionuclide therapy using patient-specific, 3-dimensional methods for SPECT reconstruction and absorbed dose calculation. J Nucl Med 46:840-849, 2005

40. Liu A, Williams L, Lopatin G, et al: A radionuclide therapy treatment planning and dose estimation system. J Nucl Med 40:1151-1153, 1999

41. Guy MJ, Flux GD, Papavasileiou P, et al: RMDP: A dedicated package for I-131 SPECT quantification, registration and patient-specific dosimetry. Cancer Biother Radiopharm 18:61-69, 2003

42. Clairand I, Ricard M, Gouriou J, et al: DOSE3D: EGS4 Monte Carlo code-based software for internal radionuclide dosimetry. J Nucl Med 40:1517-1523, 1999

43. Bielajew A, Rogers D: PRESTA: The parameter reduced electron-step transport algorithm for electron monte carlo transport. Nucl Instrum Methods B18:165-181, 1987

44. Briesmeister JF (ed): "MCNP—A General Monte Carlo N-Particle Transport Code, Version 4C," LA-13709-M, Los Alamos National Laboratory April 2000

45. Allison J, Amako K, Apostolakis J, et al: Geant4 developments and applications. IEEE Trans Nucl Sci 53:270-278, 2006

46. Lehmann J, Hartmann Siantar C, et al: Monte Carlo treatment planning for molecular targeted radiotherapy within the MINERVA system. Phys Med Biol 50:947-958, 2005

47. Sgouros G, Kolbert KS, Sheikh A, et al: Larson patient-specific dosimetry for 131I thyroid cancer therapy using 124I PET and 3-dimensional-internal dosimetry (3D-ID) software. J Nucl Med 45:1366-1372, 2004

48. DeNardo DA, DeNardo GL, O'Donnell RT, et al: Imaging for improved prediction of myelotoxicity after radioimmunotherapy. Cancer 80:2558-2566, 1997

49. Siegel JA, Lee RE, Pawlyk DA, et al: Sacral scintigraphy for bone marrow dosimetry in radioimmunotherapy. Int J Rad Appl Instrum (B) 16:553-559, 1989

50. Siegel JA, Wessels BW, Watson EE, et al: Bone marrow dosimetry and toxicity for radioimmunotherapy. Antibody Immunoconj Radiopharmacol 3:213-233, 1990

51. Lim S-M, DeNardo GL, DeNardo DA, et al: Prediction of myelotoxicity using radiation doses to marrow from body, blood and marrow sources. J Nucl Med 38:1474-1378, 1997

52. Breitz H, Fisher D, Wessels B: Marrow toxicity and radiation absorbed dose estimates from rhenium-186-labeled monocolonal antibody. J Nucl Med 39:1746-1751, 1998

53. Eary JF, Krohn KA, Press OWQ, et al: Importance of pre-treatment radiation absorbed dose estimation for radioimmunotherapy of non Hodgkin's lymphoma. Nucl Med Biol 24:635-638, 1997

54. Behr TM, Sharkey RM, Juweid ME, et al: Hematological toxicity in the radioimmunotherapy of solid cancers with ^{131}I-labeled anti-CEA NP-4 IgG[1]: Dependence on red marrow dosimetry and pretreatment. in sixth international radiopharmaceutical dosimetry symposium, Vol I: 113-125. Proceedings of May 7-10, 1996 Gatlinburg, TN, Symposium, ORAU, Jan 1999

55. Juweid ME, Zhang C-H, Blumenthal RD, et al: Prediction of hematologic toxicity after radioimmunotherapy with 131I-labeled anticarci-

lymphoma patients after radioimmunotherapy. J Nucl Med 44:1322-1329, 2003

noembryoinic antigen monoclonal antibodies. J Nuc Med 10:1609-1616, 1999

56. Wiseman GA, Kornmehl E, Leigh B, et al: Radiation Dosimetry results and safety correlations from 90Y-ibritumomab tiuxetan radioimmunotherapy for relapsed or refractory non-Hodgkin's lymphoma: Combined data from 4 clinical trials. J Nucl Med 44:465-474, 2003
57. Shen S, Meredith RF, Duan J, et al: Improved prediction of myelotoxicity using a patient-specific imaging dose estimate for non-marrow-targeting 90Y-antibody therapy. J Nucl Med 43:1245-1253, 2002
58. Siegel JA, Yeldell D, Goldenberg DM, et al: Red marrow radiation dose adjustment using plasma FLT3-l cytokine levels: Improved correlations between hematologic toxicity and bone marrow dose for radioimmunotherapy patients. J Nucl Med 44:67-76, 2003
59. Pauwels S, Barone R, Walrand S, et al: Practical dosimetry of peptide receptor radionuclide therapy with ^{90}Y-labeled somatostatin analogs. J Nucl Med 46:92S-98S, 2005 (suppl)
60. Kobe C, Eschner W, Sudbrock F, et al: Graves' disease and radioiodine therapy: Is success of ablation dependent on the achieved dose above 200 Gy? Nuklearmedizin 47:13-17, 2008
61. Smith RN, Wilson GM: Clinical trial of different doses of 131I in treatment of thyrotoxicosis. Br Med J 1:129-132, 1967
62. Becker DV, McConahey WM, Dobyns BM, et al: The results of radioiodine treatment of hyperthyroidism, in Fellinger K, Höfer R (eds): Further Advances in Thyroid Research. Vienna, Austria, Verlage der wiener Medizinischen Akademie, 1971, pp 603-609
63. Dale R, Carabe-Fernandez A: The radiobiology of conventional radiotherapy and its application to radionuclide therapy. Cancer Biother Radiopharm 20:47-51, 2005
64. Bodey RK, Flux GD, Evans PM: Combining dosimetry for targeted radionuclide and external beam therapies using the biologically effective dose. Cancer Biother Radiopharm 18:89-97, 2003
65. Barone R, Borson-Chazot F, Valkema R, et al: Patient-specific dosimetry in predicting renal toxicity with 90Y-DOTATOC: Relevance of kidney volume and dose rate in finding a dose–effect relationship. J Nucl Med 46:99S-106S, 2005
66. Dale RG: The application of the linear-quadratic dose-effect equation to fractionated and protracted radiotherapy, Br J Radiol 58:515, 1985
67. Sachs RK, Hahnfeld P, Brenner DJ: The link between low-LET dose-response relations and the underlying kinetics of damage production/repair/misrepair. Int J Radiat Biol 72:351-374, 1997
68. Lea DE, Catcheside DG: The mechanism of the induction by radiation of chromosome abberations in Tradescantia. J Genet 44:216-245, 1942
69. Barendson GW: Dose fractionation, dose-rate and iso-effect relationships for normal tissue responses. Int J Radiat Oncol Biol Phys 8:1981-1987, 1982
70. Fowler JF: The linear-quadratic formula and progress in fractionated radiotherapy. Br J Radiol 62:679-694, 1989
71. Malaroda A, Flux GD, Buffa FM, et al: Multicellular dosimetry in voxel geometry for targeted radionuclide therapy. Cancer Biother Radiopharm 18:451-461, 2003
72. O'Donoghue JA, Sgouros G, Divgi CR, et al: Single-dose versus fractionated radioimmunotherapy: Model comparisons for uniform tumor dosimetry. J Nucl Med 41:538-547, 2000
73. Prideaux AR, Song H, Hobbs RF, et al: Three-dimensional radiobiologic dosimetry: Application of radiobiologic modeling to patient-specific 3-dimensional imaging–based internal dosimetry. J Nucl Med 48:1008-1016, 2007
74. Bodey RK, Evans PM, Flux GD: Application of the linear-quadratic model to combined modality radiotherapy. Int J Radiat Oncol Biol Phys 59:228-241, 2004
75. Hall EJ: The bystander effect. Health Phys 85:31-35, 2003
76. Khan MA, Hill RP, Van Dyk J: Partial volume rat lung irradiation: An evaluation of early DNA damage. Int J Radiat Oncol Biol Phys 40:467/76, 1998
77. Sgouros G, Knox SJ, Joiner MC, et al: MIRD continuing education: Bystander and low–dose-rate effects: Are these relevant to radionuclide therapy? J Nucl Med 48:1683-1691, 2007
78. Wessels BW, Bolch WE, Bouchet LG, et al: American Association of

Physicists in Medicine: Bone marrow dosimetry using blood-based models for radiolabeled antibody therapy: A multiinstitutional comparison. J Nucl Med 45:1725-1733, 2004
79. Eschmann SM, Reischl G, Bilger K, et al: Evaluation of dosimetry of radioiodine therapy in benign and malignant thyroid disorders by means of iodine-124 and PET. Eur J Nucl Med Mol Imaging 29:760-767, 2002
80. Canzi C, Zito F, Voltini F, et al: Verification of the agreement of two dosimetric methods with radioiodine therapy in hyperthyroid patients. Med Phys 33:2860-2867, 2006
81. Carlier T, Salaun PY, Cavarec MB, et al: Optimized radioiodine therapy for Graves' disease: Two MIRD-based models for the computation of patient-specific therapeutic I-131 activity. Nucl Med Commun 27:559-566, 2006
82. Smith RN: Clinical trial of different doses of 131I in the treatment of thyrotoxicosis. Br Med J 1:129-131, 1967
83. Grosso M, Traino A, Boni G, et al: Comparison of different thyroid committed doses in radioiodine therapy for Graves' hyperthyroidism. Cancer Biother Radiopharm 20:218-223, 2005
84. Furhang EE, Larson SM, Buranapong P, et al: Thyroid cancer dosimetry using clearance fitting. J Nucl Med 40:131-136, 1999
85. Maxon HR, Thomas SR, Samaratunga RC: Dosimetric considerations in the radioiodine treatment of macrometastases and micrometastases from differentiated thyroid cancer. Thyroid 7:183-187, 1997
86. Reiners C: Radioiodine therapy of thyroid cancer. Tumordiagnostik Therapie 19:70-73, 1998
87. Benua S, Cicale NR, Sonenberg M, et al: The relation of radioiodine dosimetry to results and complications in the treatment of metastatic thyroid cancer. Am J Roentgenol Radium Ther Nucl Med 87:171-182, 1962
88. Ott RJ, Tait D, Flower MA, et al: Treatment Planning for I-131 metaiodobenzylguanidine radiotherapy of neural crest tumors using I-124 metaiodobenzylguanidine positron emission tomography. Br J Radiol 65:787-791, 1992
89. Sgouros G, Kolbert KS, Sheikh A, et al: Patient-specific dosimetry for I-131 thyroid cancer therapy using I-124 PET and 3-dimensional-internal dosimetry (3D-ID) software. J Nucl Med 45:1366-1372, 2004
90. Dorn R, Kopp J, Vogt H, et al: Dosimetry-guided radioactive iodine treatment in patients with metastatic differentiated thyroid cancer: Largest safe dose using a risk-adapted approach. J Nucl Med 44:451-456, 2003
91. Hanscheid H, Lassmann M, Luster M, et al: Iodine biokinetics and dosimetry in radioiodine therapy of thyroid cancer: Procedures and results of a prospective international controlled study of ablation after rhTSH or hormone withdrawal. J Nucl Med 47:648-654, 2006
92. Lassman M, Luste M, Hanschei H, et al: Impact of I-131 diagnostic activities on the biokinetics of thyroid remnants. J Nucl Med 45:619-625, 2004
93. Sisson JC, Avram AM, Lawson SA, et al: The so-called stunning of thyroid tissue. J Nucl Med 47:1406-1412, 2006
94. Woolfenden JM: Thyroid stunning revisited. J Nucl Med 47:1403-1405, 2006
95. Oyen WJG, Bodei L, Giammarile F, et al: Targeted therapy in nuclear medicine—current status and future prospects. Ann Oncol 18:1782-1792, 2007
96. Ron E, Doody MM, Becker DV, et al: Cancer mortality following treatment for adult hyperthyroidism. Cooperative Thyrotoxicosis Therapy Follow-up Study Group. JAMA 280:347-355, 1998
97. Hoefnagel CA: Nuclear medicine therapy of neuroblastoma. Q J Nucl Med 43:336-343, 1999
98. Matthay KK, Panina C, Huberty J, et al: Correlation of tumor and whole-body dosimetry with tumor response and toxicity in refractory neuroblastoma treated with I-131-MIBG. J Nucl Med 42:1713-1721, 2001
99. Gaze MN, Chang YC, Flux GD, et al: Feasibility of dosimetry-based high-dose I-131-meta-iodobenzylguanidine with topotecan as a radiosensitizer in children with metastatic neuroblastoma. Cancer Biotherapy Radiopharm 20:195-199, 2005
100. Monsieurs M, Brans B, Bacher K, et al: Patient dosimetry for I-131-

MIBG therapy for neuroendocrine tumours based on I-123-MIBG scans. Eur J Nucl Med Mol Imaging 29:1581-1587, 2002

101. Flux GD, Guy MJ, Papavasileiou P, et al: Absorbed dose ratios for repeated therapy of neuroblastoma with I-131 mIBG. Cancer Biother Radiopharm 18:81-87, 2003

102. Garber K: Users fear that lymphoma drugs will disappear. J Natl Cancer Inst 99:498-501, 2007

103. Wiseman GA, White CA, Sparks RB, et al: Biodistribution and dosimetry results from a phase III prospectively randomized controlled trial of Zevalin (TM) radioimmunotherapy for low-grade, follicular, or transformed B- cell non-Hodgkin's lymphoma. Crit Rev Oncol Hematol 39:181-194, 2001

104. Wahl RL, Kroll S, Zasadny KR: Patient-specific whole-body dosimetry: Principles and a simplified method for clinical implementation. J Nucl Med 39:14S-20S, 1998

105. Cremonesi M, Ferrari M, Chinol M, et al: Dosimetry in radionuclide therapies with Y-90-conjugates: the IEO experience. Q J Nucl Med 44:325-332, 2000

106. Hindorf C, Chittenden S, Causer L, et al: Dosimetry for (90)Y-DOTATOC therapies in patients with neuroendocrine tumors. Cancer Biother Radiopharm 22:130-135, 2007

107. Barone R, Walrand S, Valkema R, et al: Correlation between acute red marrow (RM) toxicity and RM exposure during Y-90-SMT487 therapy. J Nucl Med 43:1267, 2002

108. Esser JP, Krenning EP, Teunissen JJM, et al: TI Comparison of [Lu-177-DOTA(0), Tyr(3)] octreotate and [Lu-177- DOTA(0), Tyr(3)] octreotide: Which peptide is preferable for PRRT? Eur J Nucl Med Mol Imaging 33:1346-1351, 2006

109. Gotthardt M, van Eerd-Vismale J, Oyen WJG, et al: Indication for different mechanisms of kidney uptake of radiolabeled peptides. J Nucl Med 48:596-601, 2007

110. EURATOM: Health protection of individuals against the dangers of ionising radiation in relation to medical exposure: Council directive 97/43 EURATOM, 1997

111. Parthasarathy KL, Crawford ES: Treatment of thyroid carcinoma: Emphasis on high-dose ^{131}I outpatient therapy. J Nucl Med Technol 30:165-171, 2002

112. Solans R, Bosch J-A, Galofré P, et al: Salivary and lacrimal gland dysfunction (sicca syndrome) after radioiodine therapy. J Nucl Med 42:738-743, 2001

113. Siegel JA, Stabin MG, Brill AB: The importance of patient-specific radiation dose calculations for the administration of radionuclides in therapy. Cell Mol Biol 48:451-459, 2002

114. Thierens HM, Monsieurs MA, Bacher K: Patient dosimetry in radionuclide therapy: The whys and the wherefores. Nucl Med Commun 26:593-699, 2005 (review)

115. Robbins RJ, Schlumberger MJ: The evolving role of 131I for the treatment of differentiated thyroid carcinoma. J Nucl Med 46:28S-37S, 2005